Pacemaker current i_f in adult canine cardiac ventricular myocytes

Hangang Yu, Fang Chang and Ira S. Cohen*

Department of Physiology and Biophysics, Health Sciences Center, State University of New York, Stony Brook, NY 11794-8661, USA

1. Single cells enzymatically isolated from canine ventricle and canine Purkinje fibres were studied with the whole-cell patch clamp technique, and the properties of the pacemaker current, i_f, compared.

2. Steady-state i_f activation occurred in canine ventricular myocytes at more negative potentials (−120 to −170 mV) than in canine Purkinje cells (−80 to −130 mV).

3. Reversal potentials were obtained in various extracellular Na^+ (140, 79 or 37 mM) and K^+ concentrations (25, 9 or 5·4 mM) to determine the ionic selectivity of i_f in the ventricle. The results suggest that this current was carried by both sodium and potassium ions.

4. The plots of the time constants of i_f activation against voltage were 'bell shaped' in both canine ventricular and Purkinje myocytes. The curve for the ventricular myocytes was shifted about 30 mV in the negative direction. In both ventricular and Purkinje myocytes, the fully activated I–V relationship exhibited outward rectification in 5·4 mM extracellular K^+.

5. Calyculin A (0·5 μM) increased i_f by shifting its activation to more positive potentials in ventricular myocytes. Protein kinase inhibition by H-7 (200 μM) or H-8 (100 μM) reversed the positive voltage shift of i_f activation. This effect of calyculin A also occurred when the permeabilized patch was used for whole-cell recording.

6. These results indicate i_f is present in ventricular myocytes. If shifted to more positive potentials i_f could play a role in ischaemia-induced ventricular arrhythmias. The negative shift of i_f in the ventricle might play a role in differentiating non-pacing regions of the heart from those regions that pace.

The ionic mechanisms initiating the pacemaker action potential in mammalian cardiac muscle are important in understanding the regulation of heart rate. For cells to have spontaneous activity, an inward current flowing during diastole (phase 4 depolarization) is required. One of the ionic components involved in diastolic depolarization is the pacemaker current i_f. It is a time-dependent inward current activated by hyperpolarization, and is Cs^+ sensitive but largely Ba^{2+} insensitive. The i_f channel is permeable to monovalent cations, allowing both Na^+ and K^+ ions to pass through. i_f has been observed in the sino-atrial (SA) node (Yanigihara & Irisawa, 1980), frog sinus venosus (Bios & Lenfant, 1988), atrioventricular (AV) node (Noma, Irisawa, Kokobun, Kotake, Nishimura & Watanabe, 1980), atrium (Earm, Shimoni & Spindler, 1983; Zhou & Lipsius, 1992), and Purkinje fibres (DiFrancesco, 1981*a*). Although its role in pacemaking remains controversial, it contributes to the spontaneous pacemaker activity in regions such as sino-atrial node, atrium, and AV node, and is believed to be a major factor in generating the pacemaker potential in Purkinje fibres (Noble, 1984).

Both sympathetic and parasympathetic nerves play important roles in the regulation of the i_f current. Sympathetic stimulation releases β-agonists which exert a positive chronotropic effect on cardiac pacing by shifting i_f activation towards more positive potentials (Hauswirth, Noble & Tsien, 1968), thereby increasing i_f magnitude and speeding its kinetics. Vagal stimulation inhibits i_f current by shifting i_f activation towards more negative potentials (DiFrancesco & Tromba, 1988). Both sympathetic and parasympathetic stimulation alter cytosolic cAMP levels through changes in adenylyl cyclase activity; β-stimulation increases while ACh decreases the activity of this enzyme (Lindemann & Watanabe, 1990; Pappano, 1990). The positive shift of i_f activation induced by the elevation of

* To whom correspondence should be sent.

cAMP, in Purkinje fibres, is thought to be mediated by phosphorylation via cAMP-dependent protein kinase A (PKA) (Chang, Cohen, DiFrancesco, Rosen & Tromba, 1991). In the sinus node a direct action of cAMP has been proposed (DiFrancesco & Tortora, 1991). Even in the absence of β-stimulation in Purkinje fibres, H-7, a non-specific protein kinase inhibitor, can shift i_f activation to more negative potentials on the voltage axis. The important role of phosphorylation in controlling the voltage dependence of i_f activation was supported further by experiments employing the protein phosphatase inhibitor, calyculin A, which shifted i_f activation in a positive direction on the voltage axis (Yu, Chang & Cohen, 1993*a*).

In adult mammalian ventricle, i_f current has never been observed in the physiological voltage range. i_f is present, however, in chick embryonic ventricle where it begins to activate at around −50 to −60 mV, the same voltage range in which phase 4 depolarization was observed (Sperelakis, 1982; Satoh & Sperelakis, 1991). It is reported that i_f disappears during cardiac development, and this disappearance parallels the reduction of the spontaneous pacemaker activity, suggesting that the i_f current may contribute to some degree to the initiation of the pacemaker potential in chick ventricle (Satoh & Sperelakis, 1991; Brochu, Clay & Shrier, 1992).

Recently, in a preliminary report, we discovered that i_f exists in adult mammalian cardiac ventricle – a preparation that is quiescent in the normal physiological voltage range (Yu, Chang & Cohen, 1993*b*). In ventricular myocytes, i_f activated at potentials much more negative than the equilibrium potential for potassium (E_K). We did not investigate its properties in detail because only short pulses (3 s duration) were used, and steady-state i_f current was not reached.

The purpose of this paper is to characterize the properties of i_f in ventricular myocytes and compare them with the properties of i_f in canine Purkinje myocytes.

METHODS

Cell preparation

Adult dogs of either sex, weighing 18–27 kg, were killed by one injection of sodium pentobarbitone (360 mg ml^{-1}, 1 ml (4·5 kg)$^{-1}$). The heart was removed, placed in a beaker with calcium-free Tyrode solution containing (mM): NaCl, 140; $NaHCO_3$, 12; NaH_2PO_4, 0·4; $MgCl_2$, 1·6; glucose, 10; and KCl, 8 (pH 7·4), and squeezed gently to expel blood. Epicardial ventricular chunks from either side were removed using a scalpel and Purkinje fibres were dissected out. Single cells were isolated from canine Purkinje fibres and canine ventricle. The Purkinje myocytes were prepared as previously described (Cohen, Datyner, Gintant, Mulrine & Pennefather, 1987). Small chunks of ventricle (5–7 mm cubes) were dissected from the epicardium, where Purkinje myocyte contamination is least, and allowed to recover for 1 h in Ca^{2+}-free Tyrode solution at 37 °C. They were then cut into smaller pieces (1·5 × 1·5 × 3·0 mm^3) for an additional 1 h of recovery. The ventricular myocytes were dissociated using the trituration method developed earlier for Purkinje myocyte dissociation (Cohen *et al.* 1987). Oxygen and a temperature of 37 °C were provided during the dissociation in K^+ reversal solution containing (mM): KCl, 140; KH_2CO_3, 8; KH_2PO_4, 0·4; $MgCl_2$, 2; glucose, 10; taurine, 25; β-OH-butyric acid, 5; sodium pyruvate, 5 (pH 7·0). Collagenase (Type D, 0·8–1·2 mg ml^{-1}; Boehringer Mannheim) and albumin (1·6–4·0 mg ml^{-1}; Sigma) were used for successive tissue digestions. The first digestion did not yield live cells. Live cells were obtained after the second and third digestions and after trituration in the absence of collagenase. Healthy cells usually came out after the third collagenase and fourth plain K^+ reversal solution or KB medium (Isenberg & Klockner, 1982) digestion. The cells were kept in KB solution at room temperature for at least 1 h before commencing electrophysiological experiments.

Measurement of i_f and data analysis

The isolated cells were placed in a Lucite bath in which the temperature was maintained at 36 ± 0·5 °C by a temperature controller (Datyner, Gintant & Cohen, 1985). i_f currents were detected by using the whole-cell patch clamp technique with an Axopatch-1B amplifier. The pipette resistance was 2–4 MΩ when filled with solution containing (mM): NaCl, 6; potassium aspartate, 130; $MgCl_2$, 2; $CaCl_2$, 5; EGTA, 11; Na_2-ATP, 2; Na-GTP, 0·1; Na-cAMP, 0·2; and Hepes, 10 (pH adjusted to 7·2 by KOH). The external solution contained (mM): NaCl, 137·7; NaOH, 2·3; $MgCl_2$, 1; glucose, 10; Hepes, 5; KCl, 5·4; $CaCl_2$, 1·8; $MnCl_2$, 2; $CdCl_2$, 0·2; $BaCl_2$, 8 (pH 7·4). The liquid junction potential of −11 mV between the electrode tip and the cell interior (cell interior negative) was not corrected because the exchange of the pipette solution and the cell components may not have been complete (Oliva, Cohen & Mathias, 1988; Mathias, Cohen & Oliva, 1990). The divalent cations Mn^{2+} and Cd^{2+} were employed to reduce Ca^{2+} currents, which can overlap with and obscure i_f tail currents; Ba^{2+} was used to block the background K^+ current (i_{K1}) which activates and inactivates in the same voltage range as i_f. For Na^+-replacement experiments, equimolar Tris-HCl (pH 7·4) was used to replace NaCl. Calyculin A was obtained from LC Services Corporation, MA, USA. In some experiments with calyculin A the permeabilized patch technique was applied. In these experiments we used amphotericin B as described in Gao, Mathias, Cohen & Baldo (1992).

The data were recorded on an FM tape-recorder (Hewlett-Packard Co., Palo Alto, CA, USA; 3964a, speed 7/8 in s^{-1}, 600 Hz bandwidth) and simultaneously acquired by CLAMPEX software (pCLAMP, version 5.5, Axon Instruments, Inc.) for later analysis by CLAMPFIT (pCLAMP, Axon Instruments, Inc.). Data were low-pass filtered with a cut-off of 10–20 Hz and shown as means ± S.D. Each pulse was applied twice and averaged to increase the signal-to-noise ratio.

RESULTS

The i_f activation curve

We have demonstrated that i_f exists in the adult canine ventricle (Yu, Chang & Cohen, 1993*b*). It is Cs^+ sensitive and Ba^{2+} insensitive. In general, however, we did not pursue its gating properties in any detail in this earlier study because the pulses we applied did not reach steady state. Figure 1 shows the i_f current in both a ventricular and a Purkinje myocyte which we have studied for comparison. In both preparations i_f was elicited on hyperpolarization from a holding potential of −50 mV to the

voltages indicated in the figure. The pulse duration was 12 s to ensure that the i_f currents approached steady state. As shown in the activation curve (Fig. 1*C*), in this cell, ventricular i_f currents began to activate at −110 mV, slowly increased as a function of voltage, and were saturated by −180 mV. The activation curve, obtained from tail current analysis (inset in Fig. 1*A*), can be fitted by a Boltzmann function with a slope of 11·0 mV and a half-maximum activation of −134·5 mV. The mean values of slope and the mid-point for ventricular i_f activation were 8·7 ± 3·4 and −140·6 ± 12·5 mV, respectively ($n = 5$). Figure 1*B* provides results of a similar experiment in Purkinje cells. The same voltage protocol was employed. Purkinje i_f in this cell began to activate at around −80 mV and was saturated by −130 mV. The Boltzmann fit to the tail currents (inset in Fig. 1*B*) indicated a slope of 8·4 mV and a mid-point of i_f activation of −107·8 mV. The mean values of slope and mid-point for Purkinje i_f activation were 7·0 ± 1·6 and −106·1 ± 10·3 mV, respectively ($n = 5$). Figure 1*C* shows the normalized conductances calculated from tail currents (insets in Fig. 1*A* and *B*), illustrating a negative shift of ventricular i_f activation when compared with Purkinje i_f activation. Based on the mean half-activations, the negative shift of i_f activation in ventricular myocytes relative to i_f activation in Purkinje myocytes is 34·5 mV. In our earlier studies, where the mean threshold of i_f activation was used, the shift of ventricular i_f activation was −40 mV when compared with Purkinje i_f activation (Yu, Chang & Cohen, 1993*b*).

There was a very slow component of each tail current trace (see the insets of Fig. 1*A* and *B*), particularly for those recovering from very negative test pulses. This phenomenon existed in both preparations and has been described previously for i_f studies in canine Purkinje fibres (Cohen, Falk & Mulrine, 1983). Thus the tail currents following extreme hyperpolarizations did not decay entirely to baseline between pulses. We could not wait the longer time necessary because the cells would not tolerate the extremely unfavourable experimental protocol used for the extended time period required.

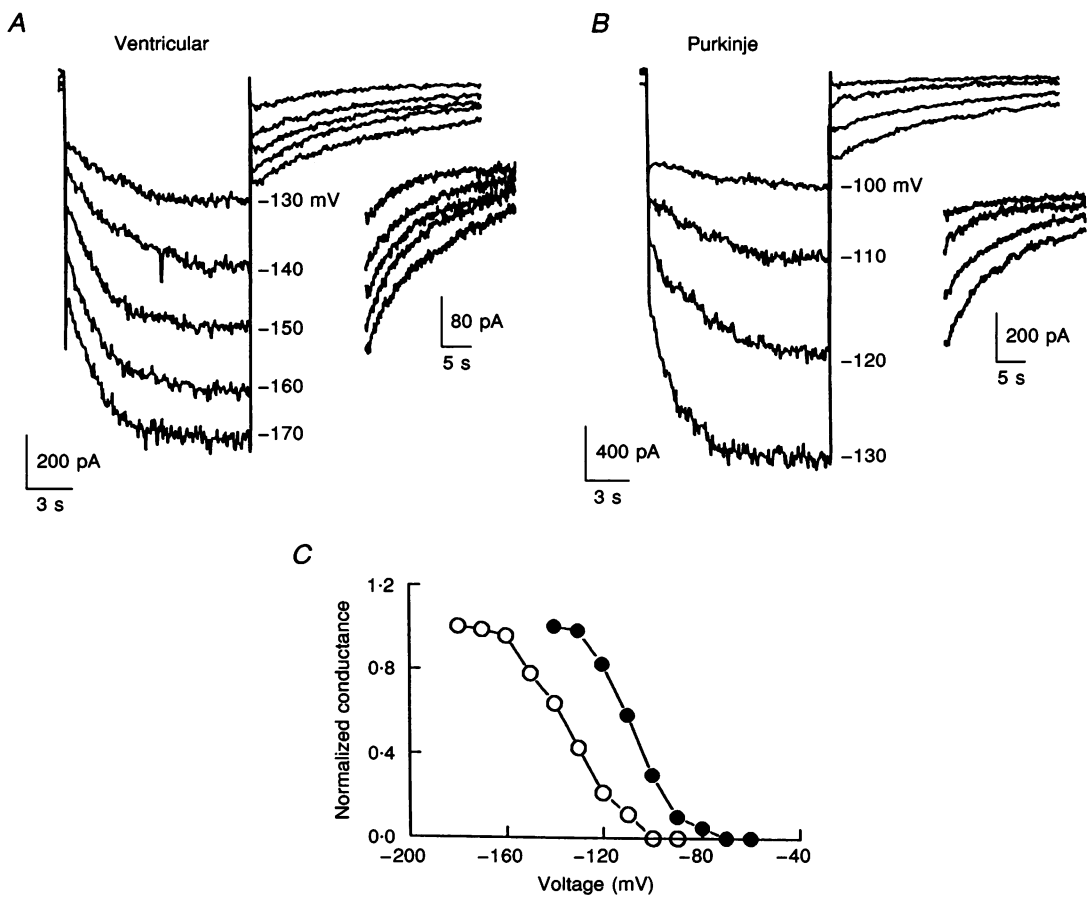

Figure 1. i_f in canine ventricular and Purkinje myocytes

The slow time-dependent inward currents were elicited upon hyperpolarization from a holding potential of −50 mV. i_f current traces are shown for the test pulses in a ventricular myocyte (*A*) and Purkinje myocyte (*B*). The mean holding currents at −50 mV were −280 pA (*A*) and −153 pA (*B*). *C*, normalized conductances obtained from tail currents shown in the insets of panels *A* (ventricular, ○) and *B* (Purkinje, ●).

Table 1. i_f reversal potentials in canine ventricular myocytes

$[Na^+]_o = 140$ mM			$[K^+]_o = 9$ mM		
$[K^+]_o$ (mM)	E_{rev} (mV)	E_K (mV)	$[Na^+]_o$ (mM)	E_{rev} (mV)	E_{Na} (mV)
5·4	−41	−93	140·0	−33	70
9·0	−33	−79	79·0	−45	55
25·0*	−13	−52	37·0*	−53	35

E_{rev}, mean observed reversal potentials; E_K and E_{Na} were predicted from the Nernst equation.
*$n = 4$; in all other cases $n = 3$.

Ionic selectivity of ventricular i_f

Before determining the reversal potential of our i_f-like ventricular current it was first necessary to demonstrate that the conductance activated by hyperpolarization was the same conductance that deactivates following the hyperpolarizing voltage clamp step. An experiment examining the envelope of tail currents is illustrated in Fig. 2. In this experiment two potentials, one positive (+25 mV) and one negative (−55 mV) to the reversal potential, were investigated. In both cases the envelope of tail currents was well fitted by the time constant derived from the current onset. Similar results were obtained from a total of six envelope tests in four ventricular myocytes. These results suggest that the tail currents we observed represented deactivation of our i_f-like current, and could be used to study its reversal potential. In our preliminary study, we found that the hyperpolarization-activated inward current displayed some K^+ selectivity when K^+ concentration was altered from 5·4 to 25 mM. However, the selectivity was far lower than that for a K^+ electrode. We have extended these initial observations by examining the Na^+ contribution to this inward current by altering extracellular sodium concentration ($[Na^+]_o$) from 140 mM to 79 and 37 mM, when $[K^+]_o$ was fixed at 9 mM. The results can be summarized as follows. In 140 mM $[Na^+]_o$ the mean reversal potentials were −41 ± 6 mV with 5·4 mM $[K^+]_o$

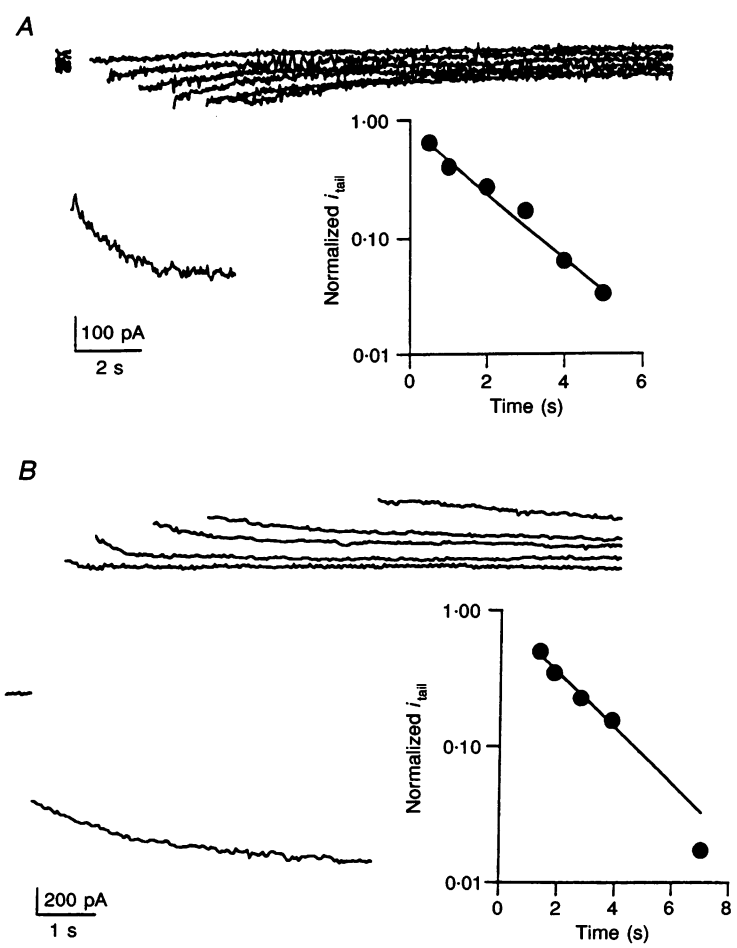

Figure 2. Two envelope tests for i_f in a single ventricular myocyte

The onset current traces were elicited by membrane hyperpolarization to −135 mV from a holding potential of −55 mV. The pulse durations for *A* were 0·5, 1·0, 2·0, 3·0, 4·0 and 5·0 s, respectively; the pulse durations for *B* were 0·5, 1·0, 2·0, 3·0 and 6·0 s, respectively. *A* shows the envelope for a test potential of −55 mV. This test potential is negative to the i_f reversal potential. The plot of the normalized envelope of the tail currents against current onset time (●) is well fitted by a single exponential function. The time constant of 1·56 s from the onset current is presented as the slope of the straight line. *B* illustrates a similar envelope for a test potential of +25 mV. This test potential is positive to the reversal potential of i_f. The plot of the normalized envelope of the tail currents against current onset time (●) is well fitted by a single exponential function. The time constant of 2·03 s from the onset current is presented as the slope of the straight line. The mean holding current at −55 mV was −168·7 pA.

($n = 3$ experiments), -33 ± 4 mV with 9 mM $[K^+]_o$ ($n = 3$), and -13 ± 5 mV with 25 mM $[K^+]_o$ ($n = 4$). In 9 mM $[K^+]_o$ the mean reversal potentials were -33 ± 4 mV with 140 mM $[Na^+]_o$ ($n = 3$), -45 ± 3 mV with 79 mM $[Na^+]_o$ ($n = 3$), and -53 ± 2 mV with 37 mM $[Na^+]_o$ ($n = 4$). Table 1 provides the mean values (E_{rev}) along with the predicted reversal potentials E_K and E_{Na} from the Nernst equation. Figure 3*A* and *B* shows raw data illustrating the effects of a change in $[K^+]_o$ on the reversal potential in two separate cells. As the extracellular potassium concentration was increased from 9 mM (Fig. 3*A*) to 25 mM (Fig. 3*B*), while $[Na^+]_o$ remained at 140 mM, the corresponding reversal potential moved from −36 mV to a more positive value (−13 mV). It indicates that this current is partially K^+ selective. It is only partially selective because the reversal potentials were much more positive than the predicted E_K in both potassium concentrations, and because the shift in the reversal potential with the change in $[K^+]_o$ was much less than the calculated change expected for a K^+-selective electrode. When $[K^+]_o$ was increased 2·8-fold (from 9 to 25 mM), the calculated shift of reversal potential for a K^+ electrode was +27 mV; however, the experimental data in Table 1 give a mean value of +20 mV. Similarly, when $[Na^+]_o$ was reduced from 140 mM (Fig. 3*A*) to 79 mM in another cell (Fig. 3*C*) while $[K^+]_o$ was kept at 9 mM, the reversal potential moved from −36 mV (Fig. 3*A*)

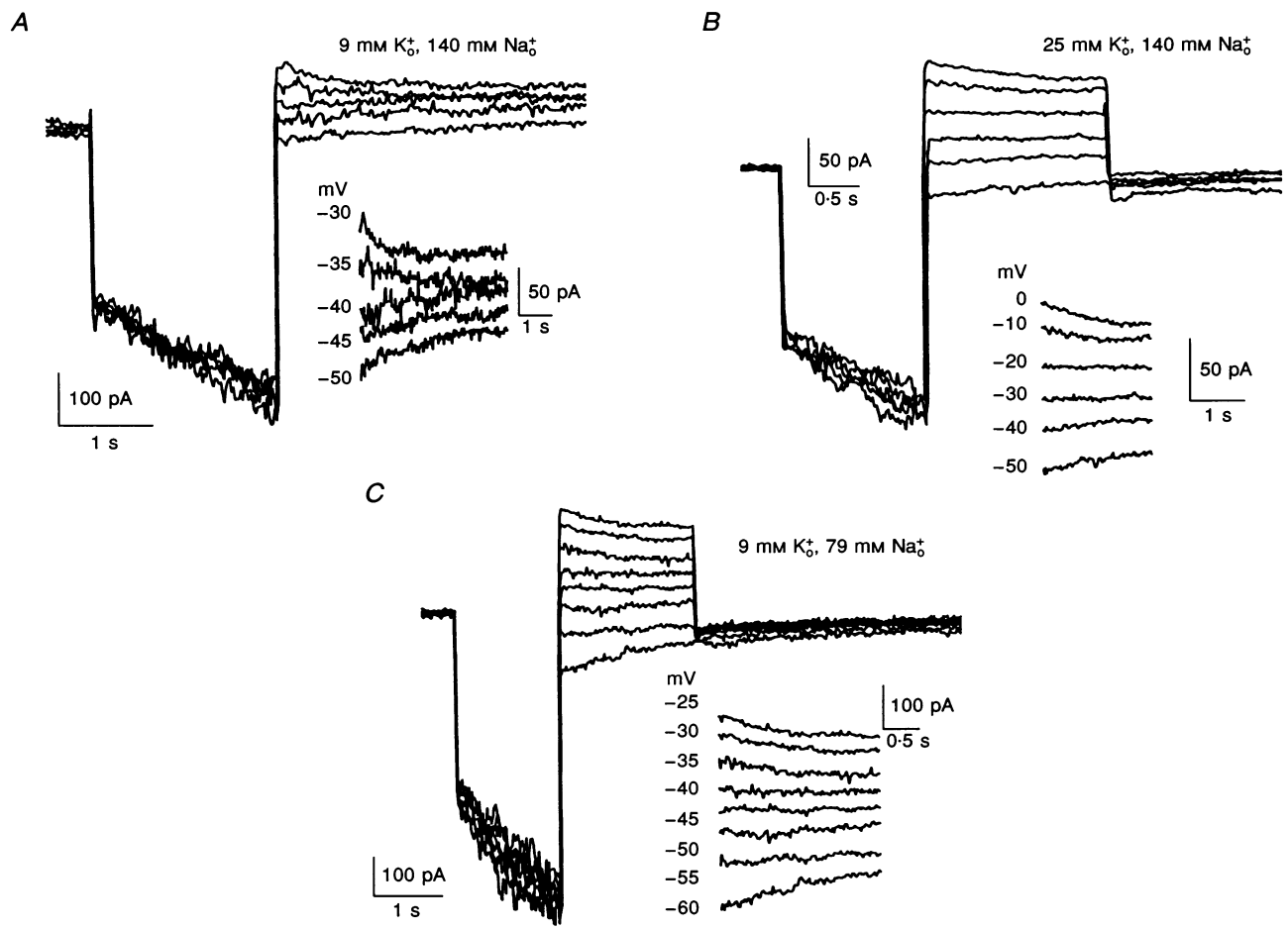

Figure 3. Reversal potential of i_f in canine ventricular myocytes

Reversal potentials in 140 mM Na_o^+ are shown in *A* with 9 mM K_o^+ and in *B* with 25 mM K_o^+. The cells were hyperpolarized to −160 mV (*A*) and −135 mV (*B*) from a holding potential of −50 mV and clamped back to the test potentials shown in the figure. The value in 9 mM K_o^+ was −36 mV and that in 25 mM K_o^+ was −13 mV. The holding current at −50 mV was −68 pA in *A* and −181 pA in *B*. The insets in panels *A*, *B* and *C* show the time-dependent tail currents expanded (with DC levels moved closer together to allow comparison). Reversal potentials in 9 mM K_o^+ with 79 mM Na_o^+ are shown in *C* and with 140 mM Na_o^+ in *A*. In *C* the cell was hyperpolarized to −170 mV from a holding potential of −60 mV and clamped back to the test potentials shown in the inset. The reversal potential in 79 mM Na_o^+ was −42 mV and that in 140 mM Na_o^+ was −36 mV. The holding current at −60 mV was −34 pA in *C*. The reversal potentials of i_f were determined by linear interpolation to zero current of the tail current amplitude on either side of the zero current level.

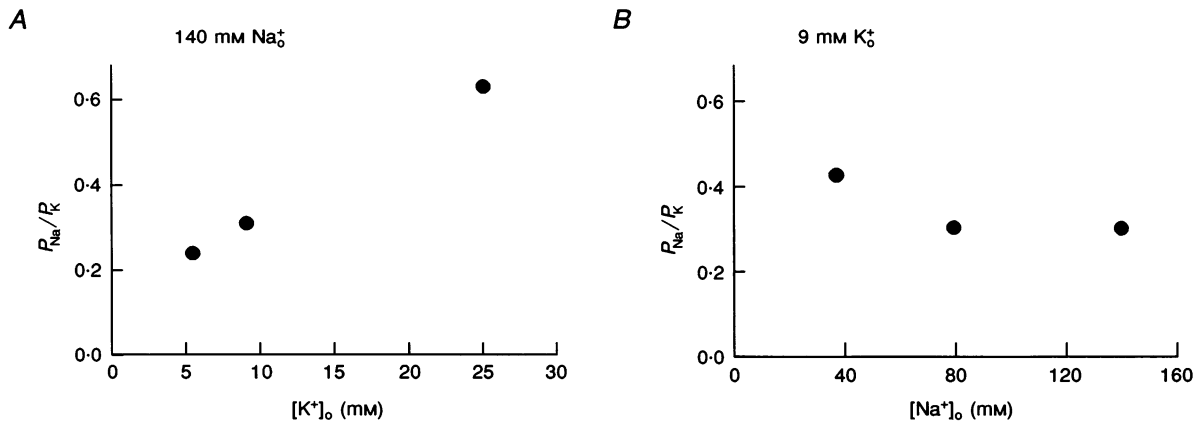

Figure 4. Ionic selectivity for i_f

The ratio of sodium ion permeation to potassium ion permeation as a function of extracellular potassium (*A*) and extracellular sodium (*B*) concentrations (see text for details).

to a more negative value (−42 mV, Fig. 3*C*), as expected for the contribution of sodium ions to this i_f current. However, it was not a pure Na^+ current. The reversal potentials were much more negative than the predicted E_{Na} in both sodium concentrations (70 mV at $[Na^+]_o$ of 140 mM and 55 mV at $[Na^+]_o$ of 79 mM), and the mean shift of reversal potential with this change in $[Na^+]_o$ (−12 mV) was less than the calculated change expected for a Na^+ electrode (−15 mV).

We also examined the ionic selectivity for i_f in another way, as shown in Fig. 4. The ratio of sodium ion to potassium ion permeation (P_{Na}/P_K) was calculated using the Goldman–Hodgkin–Katz (GHK) model (Hille, 1986) for a multiple ion channel at various extracellular potassium (Fig. 4*A*) and sodium (Fig. 4*B*) concentrations. P_{Na}/P_K changes almost linearly as $[K^+]_o$ varies within the chosen range of potassium concentrations (5·4–25 mM), but it does not show a similar sensitivity when $[Na^+]_o$ is altered.

Kinetics of ventricular i_f

Figure 5 demonstrates the time constants of i_f activation in ventricular and Purkinje myocytes (mean results in four cells, respectively). The time constants were obtained by single exponential function fitting to the 12 s-long current traces (see inset for example in a ventricular myocyte). At the beginning of i_f activation, in some cases, there existed a 'delay' in the time course of i_f currents as previously described by DiFrancesco & Ferroni (1983). The fitting was carried out by excluding this 'delay'. The activation time constant of ventricular i_f appeared to be similar to that of

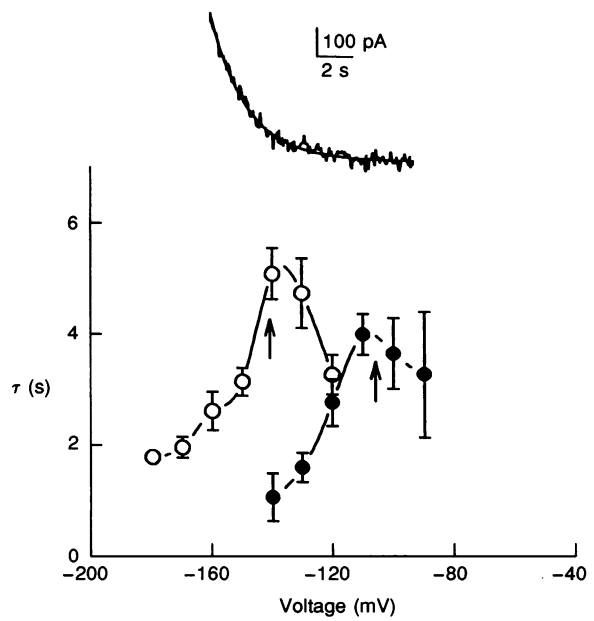

Figure 5. Time constants of i_f activation in ventricular (○) and Purkinje myocytes (●)

For each preparation, the mean results for four cells are shown. The time constants were obtained by fitting fully activated current traces with a single exponential function. The inset shows an example of a fit in a ventricular myocyte; the test pulse was to −160 mV and the time constant was 2·2 s. The arrows indicate the voltage mid-point of i_f activation in each preparation.

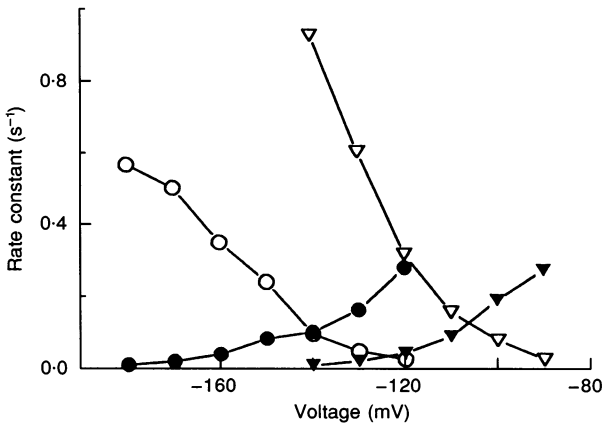

Figure 6. Rate constants for i_f activation

Rate constants for activation of i_f in ventricular (○, α; ●, β) and Purkinje (▽, α; ▼, β) myocytes, calculated by assuming a Boltzmann two-state model (see text).

Purkinje i_f, but was shifted to more negative potentials. Both sets of time constants had an approximately bell-shaped voltage dependence. The slowest time constant for activation of the ventricular i_f was shifted in the negative direction by 30 mV when compared with Purkinje myocytes. The slowest time constant was located near the voltage mid-point of the i_f activation curve in both preparations (see arrows in Fig. 5).

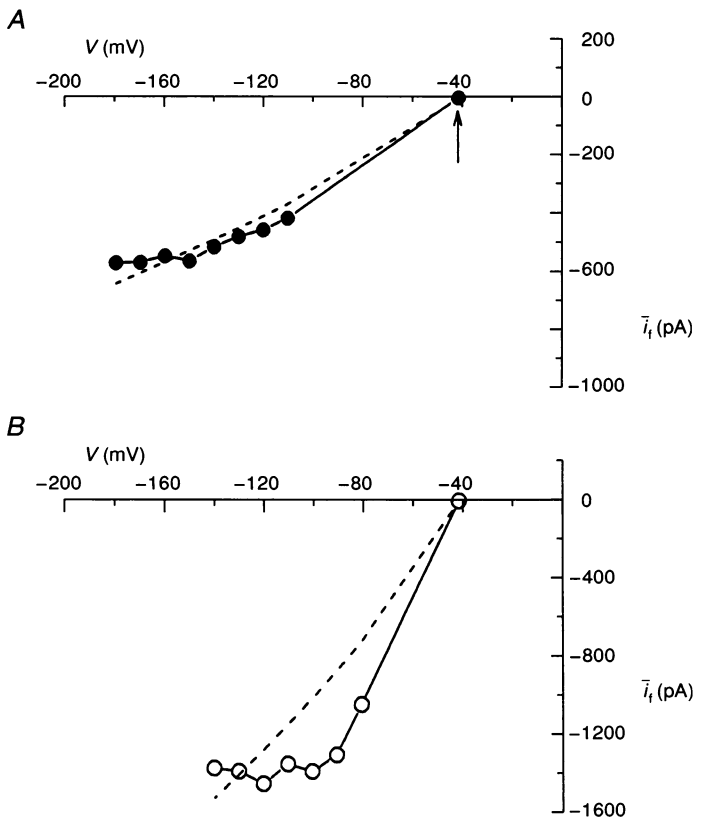

Figure 7. Fully activated I–V relationship for i_f

Fully activated I–V relationship for i_f at hyperpolarized potentials for ventricular (A) and Purkinje (B) myocytes. The data are connected by continuous lines, and are fitted by the GHK current equation (dotted lines).

Figure 6 shows the mean rate constants of i_f activation from four ventricular and four Purkinje myocytes. They were calculated by assuming a Boltzmann two-state model (closed $\underset{\beta}{\overset{\alpha}{\rightleftharpoons}}$ open, but see 'Kinetics of i_f' in Discussion) where

$$P_{o(V)} = y_\infty = \alpha/(\alpha + \beta) \quad (1)$$

and

$$\tau = 1/(\alpha + \beta), \quad (2)$$

so

$$\alpha = y_\infty/\tau \quad (3)$$

$$= (1/\tau) - \alpha, \quad (4)$$

where y_∞ is the steady-state activation (also equal to the open probability ($P_{o(V)}$) and is obtained from the tail currents. The cross-over point of α and β appeared at about −140 mV in ventricular myocytes, whereas it was around −107 mV in Purkinje myocytes (Fig. 6) near the respective mid-points of their activation curves. Besides the shift there was no significant difference in the magnitudes of the α and β values. Therefore, the kinetics of i_f activation in ventricular myocytes appear to be similar to the kinetics of i_f activation in Purkinje myocytes, except for a negative shift of their voltage dependence along the voltage axis.

Fully activated *I–V* relationship of ventricular i_f

Figure 7 shows the fully activated *I–V* relationship of ventricular i_f (Fig. 7*A*) and Purkinje i_f (Fig. 7*B*) derived from the mean data of four experiments each at extracellular potassium and sodium concentrations of 5·4 and 140 mM, respectively. The amplitude of i_f was averaged

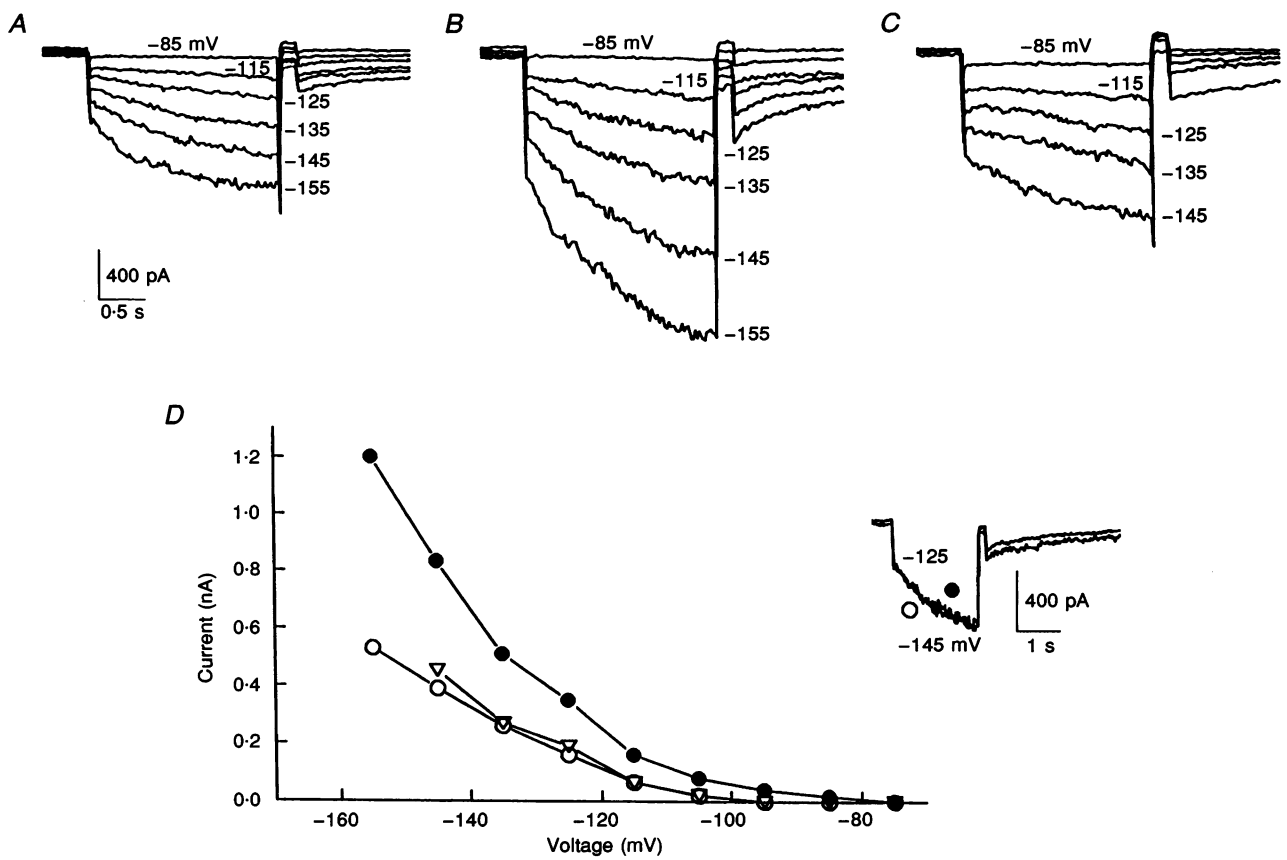

Figure 8. Effect of calyculin A on ventricular i_f

A, control solution: i_f current in a canine ventricular myocyte was activated by hyperpolarizing pulses from a holding potential of −55 mV. Current traces for the test potentials indicated are shown in the figure. The mean holding current at −55 mV was −171 pA. *B*, effect of calyculin A on i_f current in the same canine ventricular myocyte: the same voltage protocol was applied to the myocyte, and the corresponding current traces are shown. The mean holding current at −55 mV was −162 pA. *C*, control solution (washout of calyculin A): recovery of i_f current from calyculin A action is shown. The mean holding current at −55 mV was 237 pA. *D*, the isochronal (2 s) current–voltage relationships for i_f from the same cell as in *A*, *B* and *C*. The inset demonstrates that i_f current elicited during a hyperpolarization to −145 mV in control solution (○) was of similar amplitude and kinetics to that recorded at −125 mV in calyculin A-containing solution (●). ▽, recovery.

at each potential and then divided by the mean steady-state activation as indicated in the following relation:

$$\bar{i}_f = i_f(\text{on})/y_\infty, \quad (5)$$

where i_f(on) is the onset current, y_∞ is obtained from the steady-state activation curve, and the reversal potential (−41 mV at $[K^+]_o$ of 5·4 mM and $[Na^+]_o$ of 140 mM) is the value we obtained in ventricular myocytes in this solution. The arrow in Fig. 7*A* indicates the location of the reversal potential. The data are connected by a continuous line. The best fit by the GHK current equation (Hille, 1986) is indicated by a dashed line. The value of P_{Na}/P_K is 0·24 in Fig. 4*A*. Only partial fully activated *I–V* relationships were obtained because of the extreme difficulty in obtaining experimental data directly from the fully activated *I–V* protocol due to the very negative saturation potentials for ventricular i_f. The fully activated i_f current–voltage relationship outwardly rectifies (Fig. 7*A*). This non-ohmic relationship has been reported to be a property of the i_f fully activated *I–V* relationship at external potassium concentrations below 9 mM (DiFrancesco, 1981*b*). For comparison, a partial fully activated *I–V* relationship for i_f in a Purkinje myocyte is also plotted in Fig. 7*B*. The reversal potential of −41 mV (same as for ventricular i_f) was assumed. Similarly, outward rectification is observed. The dashed line shows the GHK current equation fitted with the same P_{Na}/P_K ratio as in ventricular myocytes (no value for P_{Na}/P_K fits the Purkinje data well).

Potential regulatory mechanism of i_f in ventricular myocytes

The most impressive characteristic of ventricular i_f is its extremely negative activation. When compared with Purkinje i_f, there is more than a 30 mV negative shift in i_f activation on the voltage axis. There is also a negative voltage shift of i_f activation for Purkinje myocytes compared with those from the SA node (compare van Ginneken & Giles, 1991, to Calleweart, Carmeliet & Vereecke, 1984). A possible clue to these differences may be found in studies of the actions of kinase and phosphatase inhibitors on the i_f current. The protein kinase inhibitors H-7 and H-8 have been used to show that phosphorylation

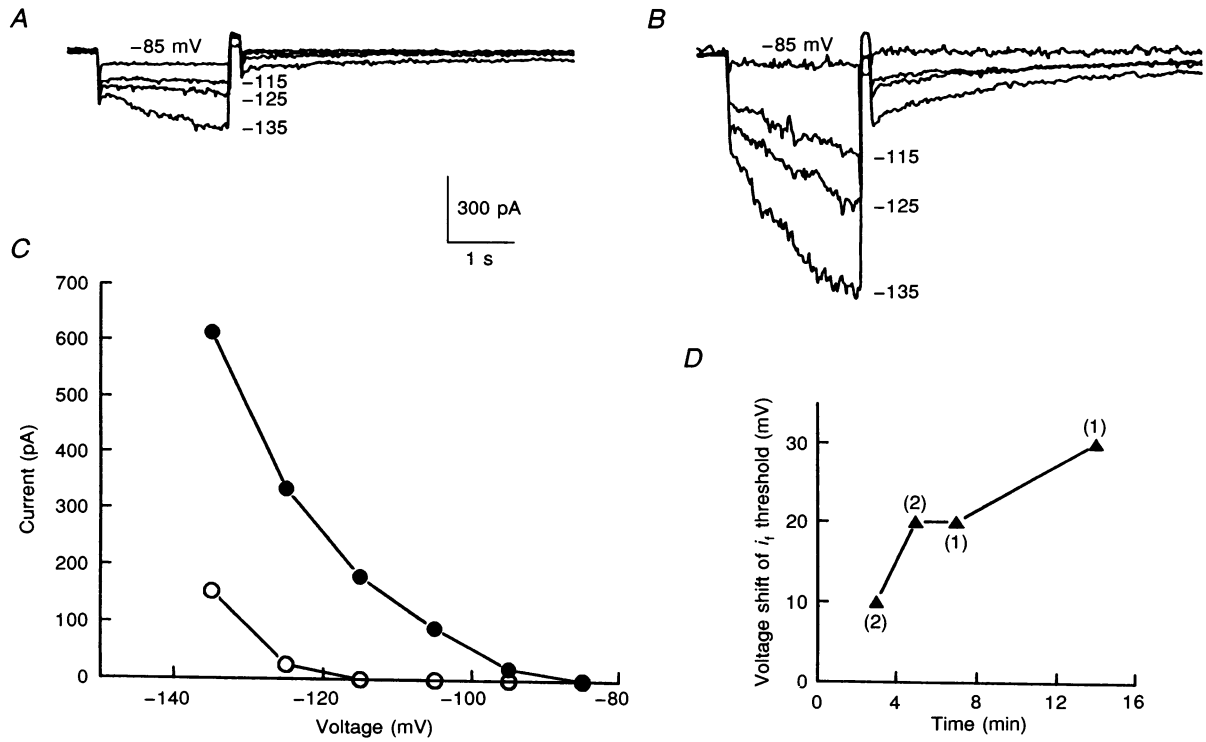

Figure 9. Effect of calyculin A on i_f in a ventricular myocyte

A, control solution: i_f current was activated by hyperpolarizing pulses from a holding potential of −55 mV. The mean holding current at −55 mV was −88 pA. *B*, effect of calyculin A on i_f current in the same ventricular myocyte: the same voltage protocol was applied to the myocyte and the corresponding current traces are shown. The mean holding current at −55 mV was −63 pA. Calyculin A was in the bath solution for 14 min. *C*, the isochronal (2 s) current–voltage relationships for i_f from the same cell as in *A* and *B* (○, control; ●, calyculin A). *D*, time-dependent shift of i_f voltage threshold during the application of calyculin A in a total of six ventricular myocytes. The number of experiments for each duration of exposure is given in parentheses in the figure.

may underlie the actions of β-agonists in canine Purkinje fibres (Chang *et al.* 1991), and H-7 could shift i_f activation to more negative potentials even without β-agonists, an action that H-8 lacked (has a higher affinity for protein kinase C). This suggested that kinase inhibition might regulate the voltage dependence of i_f activation by reducing the phosphorylation state. Alternatively, the study of the phosphatase inhibitor calyculin A on i_f activation in canine Purkinje fibres and myocytes illustrated that phosphatase inhibition may shift i_f activation to more positive voltages on the voltage axis (Yu, Chang & Cohen, 1993*a*). We decided to test the possible role of phosphorylation in determining the negative position of i_f activation in ventricular myocytes. To test this hypothesis we examined whether an increase in phosphorylation state induced by phosphatase inhibition could shift ventricular i_f activation into a more positive voltage range. Sample results are shown in Fig. 8*A*. The membrane potential was held at −55 mV and the i_f activation threshold in this cell was around −115 mV. The magnitude of i_f increased in response to more extreme hyperpolarizations down to −155 mV in the control solution. Calyculin A (0·5 μM) was applied to the bath solution for about 7 min resulting in a clear increase in i_f amplitude (Fig. 8*B*). After washout of calyculin A, i_f recovered towards its control level (Fig. 8*C*). The effects of calyculin A are largely reversible as shown in Fig. 8*D* where the isochronal *I–V* relationships were plotted. Further, after addition of calyculin A, i_f was present at potentials where no time-dependent current was visible in the control solution. Although complete activation curves were not obtainable, the isochronal current–voltage relationship (Fig. 8*D*) suggests that calyculin A shifts i_f activation to more positive potentials. Similar effects were obtained in an additional five ventricular cells, where the mean shift in the threshold for first observing i_f was +19 mV. It is interesting to notice that the effect of

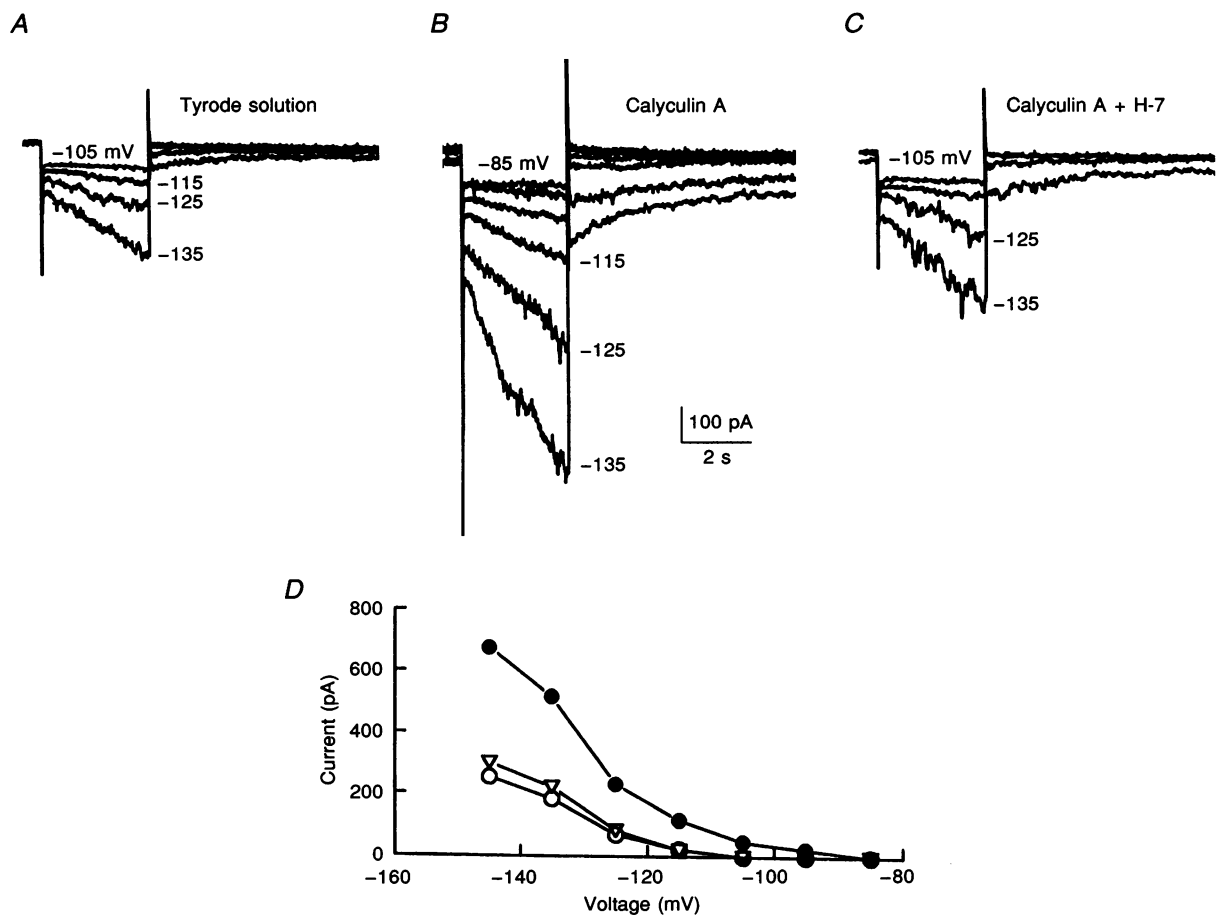

Figure 10. Effect of H-7 on ventricular i_f in the presence of calyculin A

A, i_f currents in control (Tyrode) solution. Threshold potential for i_f was −115 mV. The holding potential was −50 mV and the mean holding current at −50 mV was −240 pA. *B*, effect of calyculin A on i_f. The threshold potential for i_f was −95 mV. The mean holding current at −50 mV was −258 pA. *C*, the effect of calyculin A can be reversed by H-7. The threshold potential for i_f was again −115 mV. The mean holding current at −50 mV was −233 pA. The amplitudes of i_f current are plotted *versus* voltage for these three different conditions in *D* (○, Tyrode solution; ●, calyculin A; ▽, calyculin A + H-7).

calyculin A on i_f currents depends on the length of time of its application in most cells. Figure 9*A–C* shows a +30 mV shift when calyculin A was in the control solution for 14 min, while in Fig. 9*D* the shifts we observed in six experiments are plotted against the duration of exposure to the phosphatase inhibitor.

We next examined whether the positive shift of i_f induced by calyculin A could be reversed by kinase inhibition. Sample results are provided in Fig. 10. Figure 10*A* shows control currents recorded prior to calyculin A application. The i_f threshold was about −115 mV. Application of calyculin A shifted i_f in a more positive direction so it was now observed at −95 mV (Fig. 10*B*). When H-7, a non-specific protein kinase inhibitor, was added to the bathing Tyrode solution the positive shift of i_f induced by calyculin A was reversed (Fig. 10*C*). The amplitude of i_f current is plotted against voltage in Fig. 10*D*. These results clearly indicate that the positive activation shift induced by phosphatase inhibition (calyculin A) can be reversed by kinase inhibition. Similar results were obtained in a total of five experiments with H-8 and four with H-7. The mean threshold for i_f was −126 mV in control, −108 mV in calyculin A and −126 mV in calyculin A + kinase inhibitor (H-8 or H-7).

It is possible that phosphatase inhibition can shift i_f in the positive direction, but only if important intracellular constituents are lost due to intracellular dialysis with the whole-cell patch clamp technique. To rule out this alternative we employed the permeabilized patch with amphotericin B (Gao *et al.* 1992). Typical results are provided in Fig. 11. Control currents are provided in Fig. 11*A* and are to be compared with those with 0·5 μM calyculin A in Fig. 11*B* and washout in Fig. 11*C*. Figure 11*D* plots the i_f current amplitude for Fig. 11*A*, *B* and *C* and clearly demonstrates that a reversible positive shift of i_f activation threshold from −115 to −95 mV occurred. Similar results were obtained in a total of four experiments with amphotericin B.

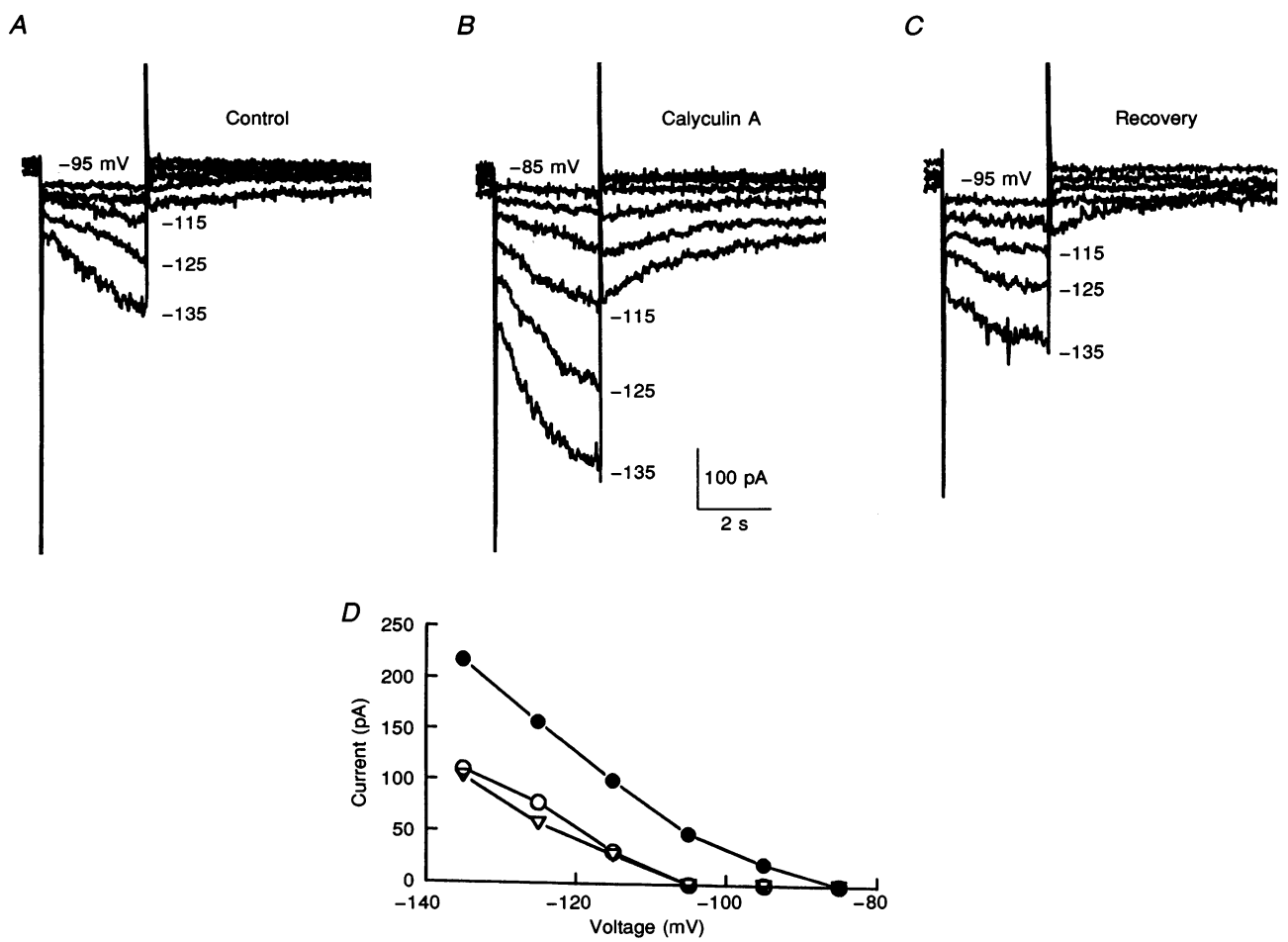

Figure 11. Effect of calyculin A on ventricular i_f with the permeabilized patch technique

i_f current appears at −115 mV in control (Tyrode) solution (*A*), but has been shifted to −95 mV in the presence of calyculin A (*B*). This effect of calyculin A was reversible on washout (*C*). The mean holding current at −50 mV was −267 (*A*), −290 (*B*) and −288 pA (*C*). The isochronal *I–V* relationships for the i_f currents of *A*, *B* and *C* are plotted in *D* for easy comparison (○, control; ●, calyculin A; ▽, recovery).

DISCUSSION

The pacemaker current, i_f, is present in the SA node and Purkinje fibres. It activates at more positive potentials in the SA node than in Purkinje fibres. i_f does not exist in the adult mammalian ventricle in the normal physiological voltage range. There were basically three hypotheses that could address the absence of i_f in adult mammalian ventricle. Hypothesis 1: the gene encoding the i_f channel could be shut off in ventricular myocytes during cardiac development; this is the easiest way to inactivate a protein that has no function. Hypothesis 2: ventricular i_f could be part of an i_f gene family, with somewhat different properties in different cardiac regions. In contrast, hypothesis 3 argues that the coding for i_f may come from a single gene which is post-translationally modified, to alter the activation of i_f in various cardiac regions, and this post-translational modification could shift i_f by some unknown mechanism to very negative potentials beyond the normal physiological range in ventricular myocytes. The evidence now for the presence of ventricular i_f activated at potentials more negative than E_K provides us with at least the following information. (a) The i_f gene is not shut off in adult cardiac ventricle. (b) There exists a different voltage dependence of i_f activation in SA node and in Purkinje myocytes. There also exists a difference in i_f activation between Purkinje and ventricular myocytes (i.e. i_f activates at more positive potentials in Purkinje myocytes). (c) Hypothesis 2 could account for this voltage gradient of i_f activation from SA node through Purkinje fibres to the working ventricle, and as we know, there is impressive heterogeneity of ion channels in different regions of the heart. Other channels like Ca^{2+}, Na^+, and K^+ channels in the heart also come from multigene families. At the same time, however, hypothesis 3 cannot be excluded, because i_f activation can be modulated by autonomic stimulation, hormones such as catecholamines, and possible basal levels of cAMP, kinases, and phosphatases (see 'Action of calyculin A on i_f' later in Discussion). (d) A question is raised about the function of the ventricular i_f since its threshold voltage of activation is more negative than E_K.

In the adult cardiac ventricular myocytes, i_f exists at very negative potentials, as partially defined in our previous report (Yu, Chang & Cohen, 1993*b*). We demonstrated that the ventricular i_f is a time-dependent inward current activated upon membrane hyperpolarization, it is Cs^+ sensitive and Ba^{2+} insensitive, and possesses some K^+ selectivity. In the present study, more quantitative characteristics of the i_f current in ventricular myocytes were investigated.

i_f activation in canine ventricular myocytes

We compared i_f activation in canine ventricular myocytes with that in canine Purkinje myocytes in the same solution and found a 30–40 mV negative voltage shift for i_f activation in ventricular myocytes. It should be noted that the threshold of i_f activation was variable from cell to cell, as has been noticed in SA node cells (DiFrancesco, 1989). In our earlier study of canine ventricular i_f activation (Yu, Chang & Cohen, 1993*b*), the voltage threshold for observing i_f activation ranged from −110 to −140 mV. During this study, an even more positive i_f activation, in one case at −105 mV, was observed. This variability of i_f activation forms one of the unique and still unexplained characteristics of i_f channels (DiFrancesco, 1989).

Ionic selectivity of i_f

Envelope tests indicated that our tail currents represented deactivation of the conductance activated on hyperpolarization. The observed reversal potentials at various $[K^+]_o$ and $[Na^+]_o$ values show that ventricular i_f is a non-selective channel that allows both Na^+ and K^+ ions to go through. We used the GHK equation to calculate the ratio of sodium permeability to potassium permeability (P_{Na}/P_K) based on the reversal potentials shown in Results. As $[K^+]_o$ increased, P_{Na}/P_K increased. However, the change in P_{Na}/P_K was small when $[Na^+]_o$ was reduced from 140 to 79 mM (Fig. 4*B*). A further reduction in $[Na^+]_o$ to 37 mM gave rise to an increase in P_{Na}/P_K. These results may reflect a possible concentration dependence of the ratio P_{Na}/P_K and limitations of the assumptions implicit in the derivation of the Goldman–Hodgkin–Katz equation applied to i_f. Alternatively, the intracellular sodium concentration may not be well controlled (Mathias *et al.* 1990). When $[K^+]_o$ is increased, Na^+–K^+ pump activity also rises and could result in a reduced $[Na^+]_i$ and a more positive E_{Na}. This possible change in E_{Na} could result in a different P_{Na}/P_K ratio. More experiments are required to rule out this potential artifact. However, it should be pointed out that in calf Purkinje fibres, when the reversal potentials of i_f measured by DiFrancesco (1981*b*) are examined, the P_{Na}/P_K ratio also varied when $[K^+]_o$ and $[Na^+]_o$ were altered.

Kinetics of i_f

The kinetics and magnitude of i_f current control the rate of spontaneous activity. In SA node cells, the time constants of i_f are close to 1 s around the middle of the activation curve (Hagiwara & Irisawa, 1989). In the present study, the mean time constant near the mid-point of the activation curve of i_f in four Purkinje cells was 4 s. The rate of spontaneous activity was higher in SA node than in Purkinje fibres. In the ventricular myocytes, however, the time constant of i_f did not appear to be slower than the time constant of i_f in Purkinje myocytes (Fig. 5), only shifted to more negative potentials on the voltage axis.

In both ventricular and Purkinje myocytes, the time course of i_f activation could not always be described by a single exponential function. A delay at the beginning of activation was frequently seen (Figs 1*B* and 8). The deactivation process also sometimes exhibited a biphasic time course. In Purkinje fibres, the kinetics of i_f have been

analysed in detail and are complex (DiFrancesco, 1985). For simplification, we have fitted the current traces by excluding the delay, if any, and employing a Boltzmann two-state model to calculate the forward (α) and backward (β) rate constants. As noted in Results, α and β values were similar in magnitude for the two preparations except for a different voltage dependence (see Fig. 6). Therefore, we may expect that ventricular i_f will behave like Purkinje i_f and contribute to pacing if it can be shifted back to the physiological voltage range of Purkinje i_f.

In conclusion, i_f is present in the ventricle, but activates at very negative potentials. Given the difference between i_f activation in SA node and Purkinje fibres, it is worth asking what mechanism (or mechanisms) might shift i_f activation in an increasingly negative direction from SA node to Purkinje fibres to working ventricle.

Action of calyculin A on i_f

In the absence of cAMP in the pipette solution, calyculin A shifted i_f activation to more positive potentials and the effect was greater when calyculin A stays in the bath for a longer time period (Fig. 9). One possible explanation for this time dependence is slow permeation due to its large size (MW 1009). Although calyculin A is membrane permeable, it takes time to cross the membrane and build up the required concentration for action (1991 Catalog Handbook, LC Services Corporation, MA, USA).

In rat aortic smooth muscle cells, Ishihara *et al.* (1989) reported an increase in activation of the L-type Ca^{2+} current by calyculin A, which resulted in an increase in $[Ca^{2+}]_i$. An elevation in $[Ca^{2+}]_i$ (from pCa 10 to 7) was found to shift i_f activation in SA node cells to more positive potentials by 13 mV (Hagiwara & Irisawa, 1989). To rule out this possibility, we strongly buffered the free $[Ca^{2+}]_i$ using a high [EGTA] (see Methods for pipette solution) and employed Mn^{2+} and Cd^{2+} in the external solution to block Ca^{2+} channels. To further confirm that the positive shift in i_f activation was due to a change in phosphorylation state, we added the non-specific kinase inhibitors H-7 or H-8, which reversed the positive shift of i_f activation induced by calyculin A. It was also important to demonstrate that the action of calyculin A on i_f could occur in the more normal intracellular conditions of the permeabilized patch. Our results showed that the shift in i_f activation during phosphatase inhibition was not an artifact of lost intracellular constituents caused by cell dialysis.

β-Agonists increase the slope of phase 4 diastolic depolarization and enhance automaticity (Toda & Shimamoto, 1968). The ionic mechanisms underlying this effect probably include a positive shift of i_f activation on the voltage axis. On the other hand, ACh decreases the slope of phase 4 diastolic depolarization and reduces spontaneous activity (del Castillo & Katz, 1955) by shifting the i_f activation curve to more negative potentials (DiFrancesco & Tromba, 1988). Both β-adrenergic and cholinergic stimulation exert their effects on i_f current by altering the intracellular cAMP levels (Chang & Cohen, 1992). Increased cAMP levels shift i_f activation in the positive direction (Tsien, 1974). In SA node cells, a direct cAMP-dependent gating was proposed (DiFrancesco & Tortora, 1991), whereas in Purkinje fibres this shift in i_f activation was thought to involve phosphorylation via cAMP-dependent protein kinase A (Chang *et al.* 1991). Recently, we have demonstrated that without β-agonists, i_f activation can be shifted in the positive direction by inhibition of phosphatase activity with a non-specific protein phosphatase inhibitor, calyculin A, in both Purkinje fibres and myocytes (Yu, Chang & Cohen, 1993*a*). The results reported here with calyculin A were similar in ventricular myocytes except that somewhat larger effects were observed.

In addition to a possible involvement of the cAMP-dependent phosphorylation in the regulation of i_f activation, $[Ca^{2+}]_i$ also affects i_f amplitude and the voltage dependence of its activation. In SA node cells, a direct gating mechanism was proposed by Hagiwara & Irisawa (1989), based on the evidence that the modulation of i_f current by $[Ca^{2+}]_i$ was not affected by inhibitors of PKC and calmodulin. In contrast, Zaza, Maccaferri, Mangoni & DiFrancesco (1991) provided evidence in favour of a non-direct gating mechanism. The obvious discrepancy may have resulted from the different cells chosen by each group (Zaza *et al.* 1991), as well as the different techniques applied (whole-cell patch clamp in Hagiwara & Irisawa, 1989; inside-out macro-patches in Zaza *et al.* 1991). Nevertheless, the potential roles of Ca^{2+}-dependent kinase (PKC) and Ca^{2+}–calmodulin-dependent kinases in the regulation of the i_f current in Purkinje and ventricular myocytes cannot be ruled out because: (1) Ca^{2+} microinjection has been shown to alter i_f current in Purkinje fibres (Isenberg, 1977); (2) H-7 (which is effective at blocking PKC) shifts i_f in the negative direction on the voltage axis, while H-8, a less effective blocker of PKC, has no such direct effect (Chang *et al.* 1991); (3) the maximal effect of cAMP-dependent PKA on i_f activation in Purkinje and ventricular myocytes is about 10 mV (Yu, Chang & Cohen, 1993*b*), which cannot fully account for the up to 30 mV positive shift in i_f activation by phosphatase inhibition in the present study (Fig. 9), further indicating that kinases other than PKA might be involved.

In summary, the regulation of i_f activation in different regions of the heart remains open to question. It is clear, however, that the equilibrium between phosphorylation and dephosphorylation is important in controlling the voltage dependence of i_f activation, at least in canine Purkinje and ventricular myocytes. Therefore, it is possible that cAMP levels may vary in different regions of the heart and that this variation may contribute to the differing voltage dependence of i_f activation in different cardiac regions

(DiFrancesco, 1993). It is also possible that protein kinase and phosphatase levels vary from SA node through Purkinje fibres to working ventricle. The negative voltage shift of i_f activation from SA node through Purkinje fibres to ventricle may be due partly to the decreasing activities of cAMP, protein kinases, and increasing activities of phosphatases.

Given the existence of i_f in ventricular myocytes and its ability to shift its threshold of activation, as a result of changes in phosphorylation state, by up to 30 mV, these results suggest that i_f might play a functional role in ventricular myocytes in unusual conditions. We therefore believe that the potential role of ventricular i_f in the genesis of ventricular arrhythmias deserves serious future experimental investigation.

Bios, P. & Lenfant, J. (1988). Existence of an i_f-like current in the isolated cells of the frog sinus venosus. *Journal of Physiology* **406**, 89*P*.

Brochu, R. M., Clay, J. R. & Shrier, A. (1992). Pacemaker current in single cells and in aggregates of cells dissociated from the embryonic chick heart. *Journal of Physiology* **454**, 503–515.

Calleweart, G., Carmeliet, E. & Vereecke, J. (1984). Single cardiac Purkinje cells: general electrophysiology and voltage-clamp analysis of the pace-maker current. *Journal of Physiology* **349**, 643–661.

Chang, F. & Cohen, I. S. (1992). Mechanism of acetylcholine action on pacemaker current (i_f) in canine Purkinje fibers. *Pflügers Archiv* **420**, 389–392.

Chang, F., Cohen, I. S., DiFrancesco, D., Rosen, M. R. & Tromba, C. (1991). Effects of protein kinase inhibitors on canine Purkinje fibre pacemaker depolarization and the pacemaker current i_f. *Journal of Physiology* **440**, 367–384.

Cohen, I. S., Datyner, N. B., Gintant, G. A., Mulrine, N. K. & Pennefather, P. (1987). Properties of sodium–potassium pump in isolated canine Purkinje myocytes. *Journal of Physiology* **383**, 251–267.

Cohen, I. S., Falk, R. T. & Mulrine, N. K. (1983). Actions of barium and rubidium on membrane currents in canine Purkinje fibres. *Journal of Physiology* **338**, 589–612.

Datyner, N. B., Gintant, G. A. & Cohen, I. S. (1985). Versatile temperature controlled tissue bath for studies of isolated cells using an inverted microscope. *Pflügers Archiv* **403**, 318–323.

del Castillo, J. & Katz, B. (1955). Production of membrane potential changes in the frog's heart by inhibitory nerve impulses. *Nature* **175**, 1035.

DiFrancesco, D. (1981*a*). A new interpretation of the pacemaker current in calf Purkinje fibres. *Journal of Physiology* **314**, 359–376.

DiFrancesco, D. (1981*b*). A study of the ionic nature of the pacemaker current in calf Purkinje fibres. *Journal of Physiology* **314**, 377–393.

DiFrancesco, D. (1985). The cardiac hyperpolarizing-activated current, i_f. Origins and developments. *Progress in Biophysics and Molecular Biology* **46**, 163–183.

DiFrancesco, D. (1989). Current i_f and its contribution to cardiac pacemaking. In *Neuronal and Cellular Oscillators*, ed. Jacklet, J. W., pp. 31–57. Marcel Dekker, Inc., New York, Basel.

DiFrancesco, D. (1993). Pacemaker mechanisms in cardiac tissue. *Annual Review of Physiology* **55**, 455–472.

DiFrancesco, D. & Ferroni, A. (1983). Delayed activation of the cardiac pacemaker current and its dependence on conditioning pre-hyperpolarization. *Pflügers Archiv* **396**, 265–267.

DiFrancesco, D. & Tortora, P. (1991). Direct activation of cardiac 'pacemaker' (i_f) channels by intracellular cyclic-AMP. *Nature* **351**, 145–147.

DiFrancesco, D. & Tromba, C. (1988). Inhibition of the hyperpolarization-activated current (i_f) induced by acetylcholine in rabbit sino-atrial node myocytes. *Journal of Physiology* **405**, 477–491.

Earm, Y. E., Shimoni, Y. & Spindler, A. (1983). A pacemaker-like current in the sheep atrium and its modulation by catecholamines. *Journal of Physiology* **342**, 569–590.

Gao, J., Mathias, R. T., Cohen, I. S. & Baldo, G. J. (1992). Isoprenaline, Ca^{2+} and the Na^+–K^+ pump in guinea-pig ventricular myocytes. *Journal of Physiology* **449**, 689–704.

Hagiwara, N. & Irisawa, H. (1989). Modulation by intracellular Ca^{2+} of the hyperpolarization-activated inward current in rabbit sino-atrial node cells. *Journal of Physiology* **409**, 121–141.

Hauswirth, O., Noble, D. & Tsien, R. (1968). Adrenaline: mechanism of action on the pacemaker potential in cardiac Purkinje fibers. *Science* **162**, 916–917.

Hille, B. (1986). *Ionic Channels of Excitable Membranes*. Sinauer Associates Inc., Sunderland, MA, USA.

Isenberg, G. (1977). Cardiac Purkinje fibres – $[Ca^{2+}]_i$ controls the potassium permeability via the conductance components g_{K1} and g_{K2}. *Pflügers Archiv* **371**, 77–85.

Isenberg, G. & Klockner, U. (1982). Calcium currents in bovine ventricular myocytes are fast and of large amplitude. *Pflügers Archiv* **395**, 30–41.

Ishihara, H., Ozaki, H., Sato, K., Hori, M., Karaki, H., Watabe, S., Kato, Y., Fusetani, N., Hashimoto, K., Uemura, D. & Hartshorne, D. J. (1989). Calcium-independent activation of contractile apparatus in smooth muscle by calyculin-A. *Journal of Pharmacology and Experimental Therapeutics* **250**, 388–396.

Lindemann, J. P. & Watanabe, A. M. (1990). Sympathetic control of cardiac electrical activity. In *Cardiac Electrophysiology: From Cell to Bedside*, ed. Zipes, D. P. & Jalife, J., pp. 277–283. Saunders, Philadelphia, PA, USA.

Mathias, R. T., Cohen, I. S. & Oliva, C. (1990). Limitations of the whole cell patch clamp technique in the control of intracellular concentrations. *Biophysical Journal* **58**, 759–770.

Noble, D. (1984). The surprising heart: a review of recent progress in cardiac electrophysiology. *Journal of Physiology* **353**, 1–50.

Noma, A., Irisawa, H., Kokobun, S., Kotake, H., Nishimura, M. & Watanabe, Y. (1980). Slow current systems in the A–V node of the rabbit heart. *Nature* **285**, 228–229.

Oliva, C., Cohen, I. S. & Mathias, R. T. (1988). Calculation of time constants for intracellular diffusion in whole cell patch clamp configuration. *Biophysics Journal* **54**, 791–799.

Pappano, A. (1990). Parasympathetic control of cardiac electrical activity. In *Cardiac Electrophysiology: From Cell to Bedside*, ed. Zipes, D. P. & Jalife, J., pp. 271–276. Saunders, Philadelphia, PA, USA.

Satoh, H. & Sperelakis, N. (1991). Identification of the hyperpolarization-activated inward current in young embryonic chick heart myocytes. *Journal of Developmental Physiology* **15**, 247–252.

Sperelakis, N. (1982). Pacemaker mechanisms in myocardial cells during development of embryonic chick hearts. In *Cardiac Rate and Rhythm*, ed. Bouman L. N. & Jongsma H. J., pp. 129–165. Martinus Nijhoff Publishers, The Hague.

TODA, N. & SHIMAMOTO, K. (1968). The influence of sympathetic stimulation on transmembrane potentials in the SA node. *Journal of Pharmacology and Experimental Therapeutics* **159**, 298–305.

TSIEN, R. W. (1974). Mode of action of chronotropic agents in cardiac Purkinje fibers. *Journal of General Physiology* **64**, 320–342.

VAN GINNEKEN, A. C. G. & GILES, W. (1991). Voltage clamp measurements of the hyperpolarization-activated current I_f in single cells from rabbit sino-atrial node. *Journal of Physiology* **434**, 57–83.

YANIGIHARA, K. & IRISAWA, H. (1980). Inward current activated during hyperpolarization in the rabbit sinoatrial node cell. *Pflügers Archiv* **385**, 11–19.

YU, H., CHANG, F. & COHEN, I. S. (1993*a*). Phosphatase inhibition by calyculin A increases I_f in canine Purkinje fibers and myocytes. *Pflügers Archiv* **422**, 614–616.

YU, H., CHANG, F. & COHEN, I. S. (1993*b*). Pacemaker current exists in ventricular myocytes. *Circulation Research* **72**, 232–236.

ZAZA, A., MACCAFERRI, G., MANGONI, M. & DIFRANCESCO, D. (1991). Intracellular calcium does not directly modulate cardiac pacemaker (i_f) channels. *Pflügers Archiv* **419**, 662–664.

ZHOU, Z.-F. & LIPSIUS, S. L. (1992). Properties of the pacemaker current (I_f) in latent pacemaker cells isolated from cat right atrium. *Journal of Physiology* **453**, 503–523.

Acknowledgements

We would like to thank Ms Joan Zuckerman for the cell dissociation, Judy Samarel for polylysine slide and electrode preparation, and Dr Jianmin Cui for thoughtful criticism. This work was supported by NIH grants HL20558 and PPG HL28958.

Received 25 November 1993; accepted 1 December 1994.